SAGE-Var: An Infrared Survey of Variability in the Magellanic Clouds

D. Riebel

Department of Physics, United States Naval Academy, 572C Holloway Road, Annapolis,
MD 21402, USA

`riebel.d@gmail.com`

M. L. Boyer

Observational Cosmology Laboratory, Code 665, NASA Goddard Space Flight Center,
Greenbelt, MD 20771, USA

S. Srinivasan

Academia Sinica, Institute of Astronomy and Astrophysics, P.O. Box 23-141, Taipei 10617,
Taiwan

P. Whitelock

Astrophysics, Cosmology and Gravity Centre, Astronomy Department, University of Cape
Town, Rondebosch 7701, South Africa

South African Astronomical Observatory, PO Box 9, Observatory 7935, South Africa

M. Meixner

Space Telescope Science Institute, 3700 San Martin Drive, Baltimore, MD 21218, USA

Department of Physics and Astronomy, The Johns Hopkins University, 3400 N. Charles St.
Baltimore, MD 21218, USA

B. Babler

Department of Astronomy, University of Wisconsin-Madison, Madison, WI 53706, USA

M. Feast

Astrophysics, Cosmology and Gravity Centre, Astronomy Department, University of Cape Town, Rondebosch 7701, South Africa
South African Astronomical Observatory, PO Box 9, Observatory 7935, South Africa

M. A. T. Groenewegen

Royal Observatory of Belgium, Ringlaan 3, B-1180 Brussels, Belgium

Y. Ita

Astronomical Institute, Graduate School of Science, Tohoku University, 6-3 Aramaki Aoba, Aoba-ku, Sendai, Miyagi 980-8578, Japan

M. Meade

Department of Astronomy, University of Wisconsin-Madison, Madison, WI 53706, USA

B. Shiao

Space Telescope Science Institute, 3700 San Martin Drive, Baltimore, MD 21218, USA

B. Whitney

Department of Astronomy, University of Wisconsin-Madison, Madison, WI 53706, USA

Received ______________________; accepted ______________________

ABSTRACT

We present the first results from the SAGE-Var program, a follow on to the *Spitzer* legacy program *Surveying the Agents of Galaxy Evolution* (SAGE; Meixner et al. 2006). We obtained 4 epochs of photometry at 3.6 & 4.5 μm covering the bar of the Large Magellanic Cloud (LMC) and the central region of the Small Magellanic Cloud (SMC) in order to probe the variability of extremely red sources missed by variability surveys conducted at shorter wavelengths, and to provide additional epochs of observation for known variables. Our 6 total epochs of observations allow us to probe infrared variability on 15 different timescales ranging from ∼20 days to ∼5 years. Out of a full catalog of 1 717 554 (LMC) and 457 760 (SMC) objects, we find 10 (LMC) and 6 (SMC) large amplitude AGB variables without optically measured variability owing to circumstellar dust obscuration. The catalog also contains multiple observations of known AGB variables, type I and II Cepheids, eclipsing variables, R CrB stars and young stellar objects which will be discussed in following papers. Here we present infrared Period-Luminosity (PL) relations for classical Cepheids in the Magellanic Clouds, as well as improved PL relationships for AGB stars pulsating in the fundamental mode using mean magnitudes constructed from 6 epochs of observations.

1. INTRODUCTION

The study of stellar variability has had a wide-ranging impact on astronomy and cosmology. Recent variable star surveys such as the MAssive Compact Halo Object search (MACHO; Alcock et al. 1997) and the Optical Gravitational Lensing Experiment (OGLE; Udalski et al. 1997) have generated catalogs of tens of thousands of variable stars of numerous classes in the Magellanic Clouds. However, like most ground-based variability surveys, both of these were performed at visible wavelengths, and therefore miss the reddest variable sources, such as dust-enshrouded, highly evolved Asymptotic Giant Branch (AGB) stars, which are nearly invisible except in the infrared (IR). AGB stars are unstable, and exhibit variability on timescales of hundreds of days (Vassiliadis & Wood 1993). Due to this, they are also classified as Long period Variables (LPVs). There are several surveys that monitored LPVs at near-IR wavelengths in the Magellanic Clouds (J, H, and K-bands; Ita et al. 2002; Whitelock et al. 2003), but even these can still miss the dustiest sources. The pulsation properties of the heavily enshrouded (and most evolved) AGB stars are therefore not well understood. This problem can be addressed with IR monitoring at wavelengths longer than $3\,\mu$m, but there are very few examples of mid-IR monitoring surveys in any galaxy. Le Bertre (1992, 1993) obtained light curves at 1–20 μm of $\sim$60 O- and C-rich AGB stars in our own galaxy and found that while pulsation amplitudes generally decrease into the mid-IR, circumstellar dust can cause amplitudes to increase again at $\lambda > 3\,\mu$m. In M33, McQuinn et al. (2007) obtained 5-epochs of imaging at 3.6, 4.5, 5.8, and $8\,\mu$m and found that the pulsation amplitude tends to increase with color, but that this relationship may break down at the longest wavelengths. In the Magellanic Clouds and other nearby dwarf galaxies, only 2–3 epochs of imaging is available at $\lambda > 3\,\mu$m (Polsdofer et al. 2015; Vijh et al. 2009; Boyer et al. 2015a,b). While these surveys can detect flux changes in a large fraction of the dustiest stars, they cannot place stringent limits on the pulsation periods or amplitudes in the infrared. In order to explore the variability of these reddest sources, which dominate the mass return to the interstellar medium (ISM) from evolved stars (Riebel et al. 2012), we used the *Spitzer Space Telescope* to survey the bar regions of the LMC and SMC at 3.6 and $4.5\,\mu$m. SAGE-Var represents the first large scale variability survey at such red wavelengths. While our original focus was the reddest AGB stars, we have detected over 2,700 IR variables in the Clouds of many classes.

This paper is organized as follows: In § 2 we detail the observational strategy and catalog construction for the SAGE-Var program. In § 2.4 we discuss the classification of objects found in our survey. In § 3.1, we report variability detections for several AGB stars without OGLE or MACHO periods. Many of these sources were identified by the WISE survey as potential variables, and we confirm this result. In § 3.3 we present IR Period-Luminosity (PL) relations for LPVs (§ 3.3.1) and Cepheids (§ 3.3.2). Our conclusions are presented in § 4.

2. THE DATA

2.1. Observations

The 4 epochs of SAGE-Var observations (*Spitzer* PID 70020) were taken over a 10 month period, between August 2010 and June 2011 (see Table 1). Each epoch is a $3.7^\circ \times 1.5^\circ$ (LMC, Figure 1) or $1.7^\circ \times 1.7^\circ$ (SMC, Figure 2) mapping of the bar region of the galaxy, using both the [3.6] and [4.5] bands of the *Spitzer* warm mission. All frames were taken as 12 second exposures using the IRAC High Dynamic Range (HDR) mode, which also produces short 0.6 sec exposures in order to mitigate the effects of saturation for the brightest sources. This exposure mode was chosen to provide uniformity with the previous two epochs of the SAGE-LMC (Meixner et al. 2006) and SAGE-SMC (Gordon et al. 2011) surveys. The scheduling of our observations was determined using a Madore & Freedman (2005) power-law cadence with an index of 0.99, taking into account the original two SAGE epochs. Including these two original epochs, our 6 total epochs of observations allow us to probe variability on 15 different timescales (see § 2.3).

Table 1. Observation dates

Epoch	Date	Julian Date
	LMC:	
Epoch 1:	2005 Jul 20	2453572
Epoch 2:	2005 Oct 28	2453672
Epoch 3:	2010 Aug 17	2455426
Epoch 4:	2010 Sep 10	2455450
Epoch 5:	2010 Dec 25	2455556
Epoch 6:	2011 Apr 27	2455679
	SMC:	
Epoch 1:	2008 Jun 15	2454633
Epoch 2:	2008 Sep 19	2454729
Epoch 3:	2010 Aug 17	2455426
Epoch 4:	2010 Sep 12	2455452
Epoch 5:	2010 Dec 24	2455555
Epoch 6:	2011 Jun 16	2455729

Note. — Dates of the 6 epochs of observations of the SAGE-Var project, including the 2 epochs of the original SAGE-LMC and SAGE-SMC programs (Epochs 1 & 2). The dates listed for the original two epochs of observations are the approximate midpoints of the ∼5 day observation periods, while later epochs were executed during a single 24-hour period.

2.2. Data Reduction

The SAGE-Var data were processed using a pipeline developed at the University of Wisconsin for the GLIMPSE survey (Benjamin et al. 2003), and was the same pipeline used for processing the original SAGE-LMC and SAGE-SMC observations. The Wisconsin pipeline corrects for numerous observational artifacts such as stray light, column pulldown, banding, and bad pixels (Hora et al. 2004). In addition, the individual frames are mosaicked, and point sources identified. During catalog construction (§ 2.3), the point source lists are also position matched to 2MASS JHK_s photometry. The 2MASS bands have been dereddened to account for interstellar extinction. The reddening coefficients used for the LMC can be found in Table 1 of Riebel et al. (2012). The photometry for the more distant SMC was dereddened using a value of $E_{B-V} = 0.04$ mag (Harris & Zaritsky 2004; Schlegel et al. 1998) and the prescription of Glass et al. (1999, pp.109–111).

The pipeline provides 1σ photometric uncertainty in each band, plotted as a function of source magnitude in Figure 3. Throughout this paper, we take these 1σ errors as the uncertainties in our photometry. Our fluxes were transformed into magnitudes using zero points (magnitude units) of 6.12 for [3.6] and 5.63 for [4.5].

2.3. Catalog Construction

The initial data product was a 'full' point source list, without cosmic ray screening. These artifacts were removed from the catalog by matching the full lists to the SAGE mosaic photometry archive [1] using a $2''$ matching radius. The mosaic archives of the original SAGE surveys were constructed by co-adding and re-reducing the photometry from

---

[1] `http://data.spitzer.caltech.edu/popular/sage/20090922_enhanced/documents/SAGEDataProductsDescription_Sep09.pdf`

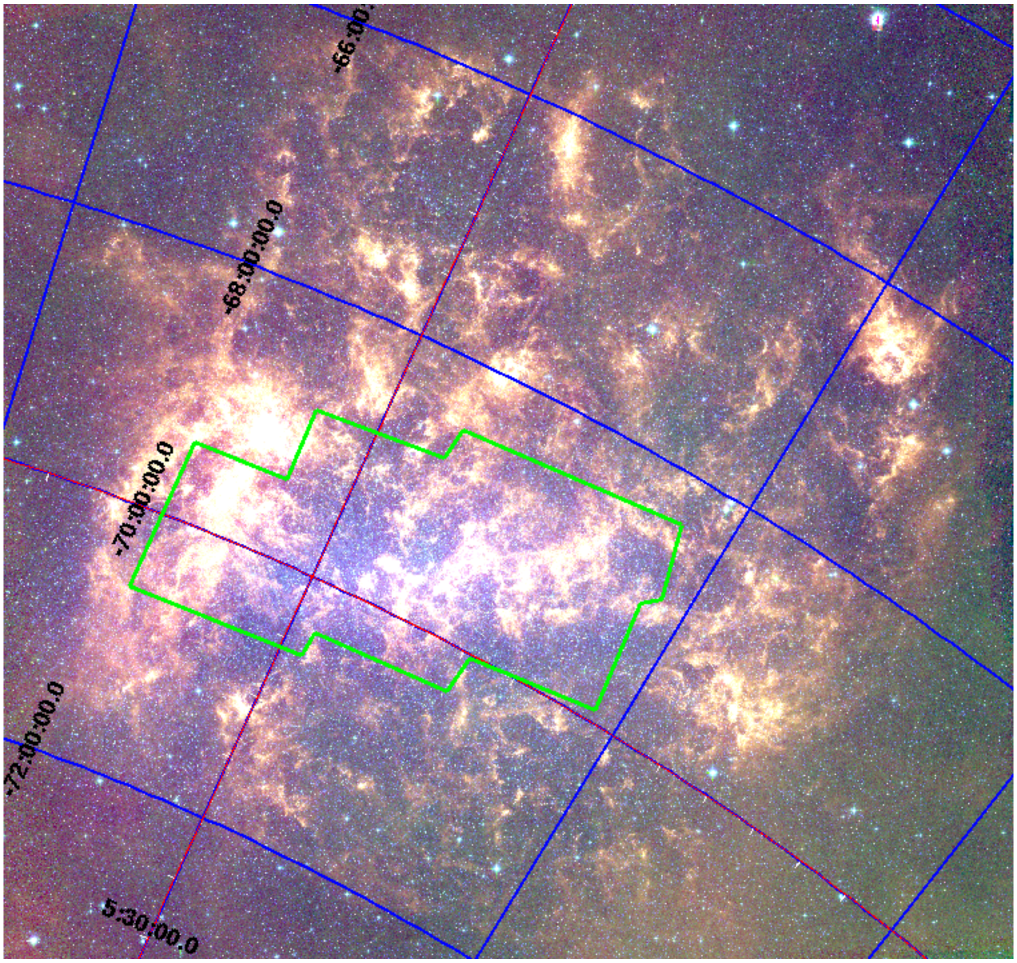

Fig. 1.— Three-color image of the LMC (red: 8.0 μm, green: 5.8 μm, blue: 3.6 μm) showing the footprint of the SAGE-Var observations in green, focused on the stellar bar region of the galaxy.

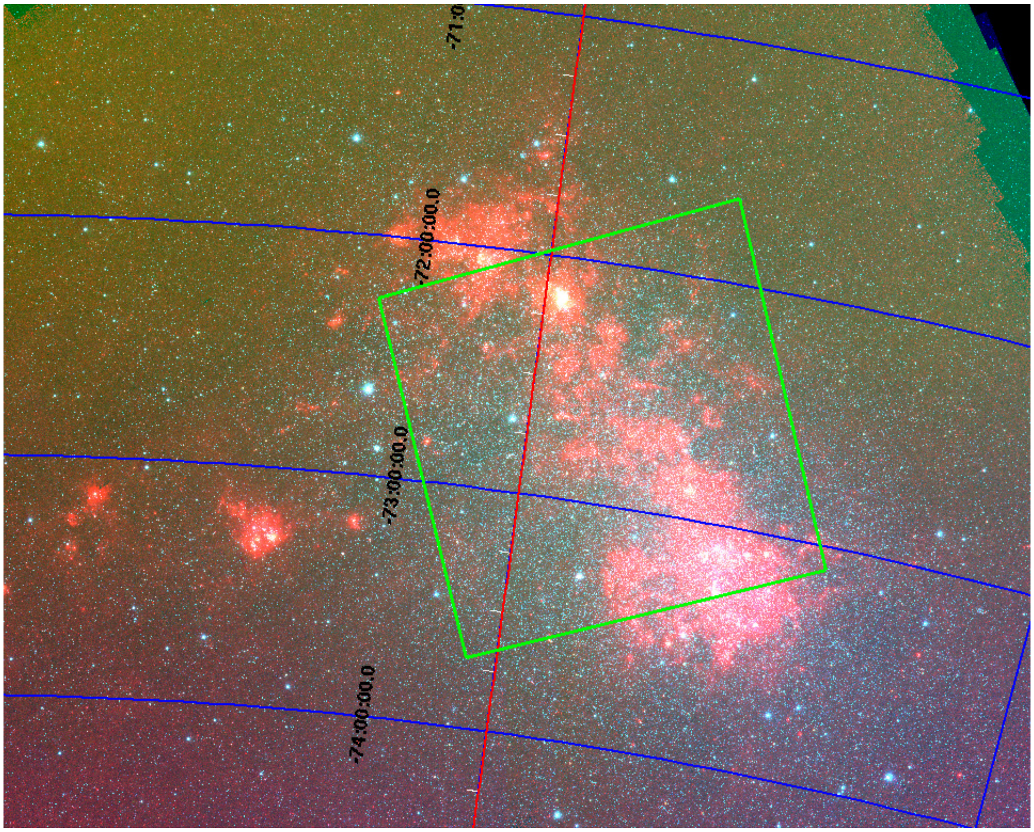

Fig. 2.— Three-color image of the SMC (red: 24 μm, green: 4.5 μm, blue: 3.6 μm) showing the footprint of the SAGE-Var observations in green, focused on the main stellar locus of the galaxy.

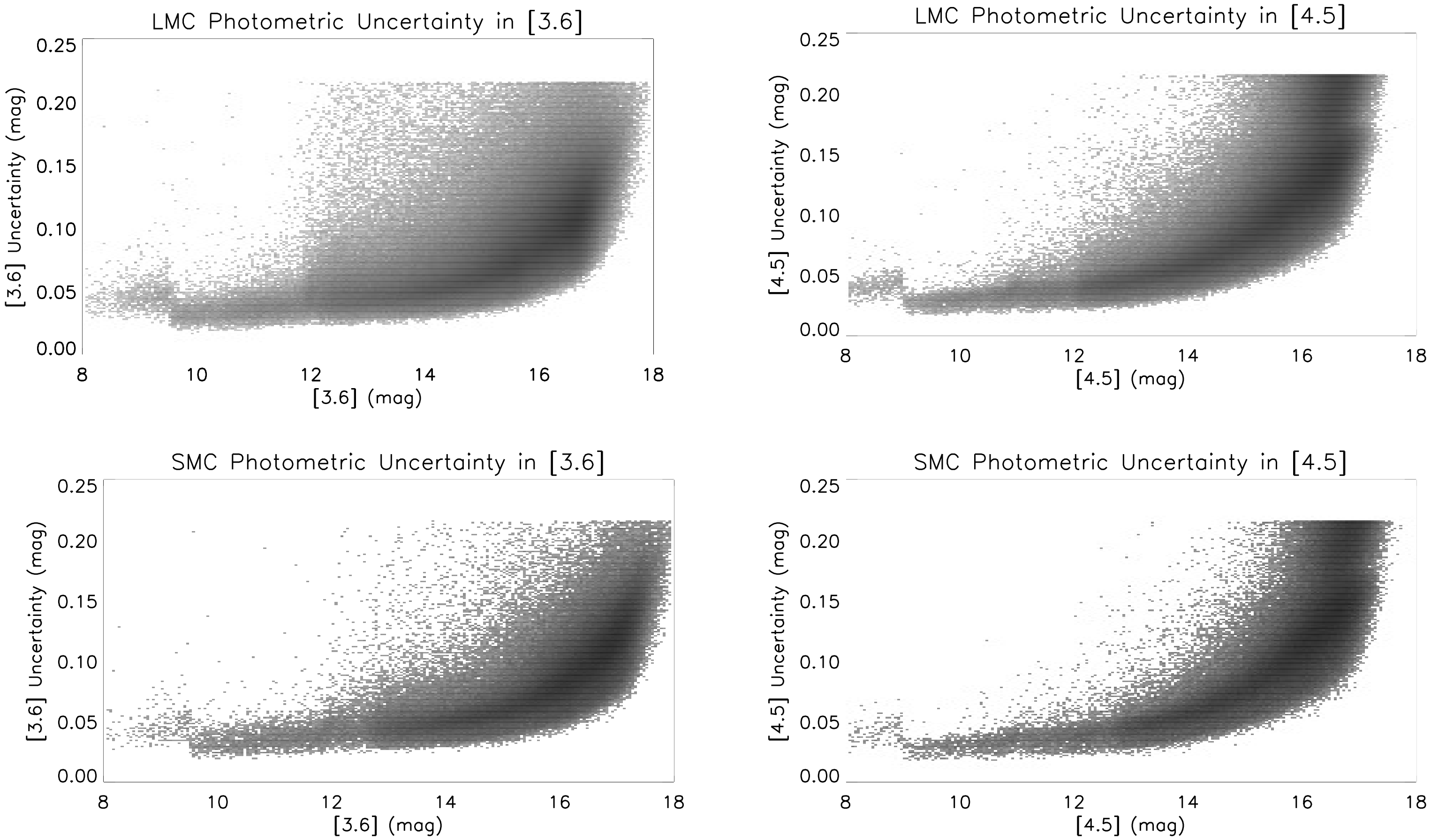

Fig. 3.— Each plot shows the 1σ uncertainty produced from the Wisconsin pipeline as a function of source magnitude for the entire SAGE-Var dataset as a Hess diagram. The top row shows the data from the LMC ([3.6] on the left, [4.5] on the right), while the bottom row shows the SMC data.

the original two SAGE Epochs. The archives are deeper, more complete, and of higher signal-to-noise (S/N) than the SAGE-Var data due to the greater exposure time of the mosaic photometry (up to ∼50 s per pixel compared to 12 s) and the fact that the original surveys were performed during the cold phase of the *Spitzer* mission whereas the SAGE-Var observations were taken after the liquid helium cryogen aboard *Spitzer* was exhausted. The higher operating temperature of the *Spitzer* instruments restricts our observations to only the shortest IRAC wavelengths, and lends additional thermal noise to our images. Due to their greater depth and quality, the SAGE mosaic archives serve as a 'truth field' for the SAGE-Var full source lists, providing a more thorough list of actual astronomical sources while screening out instrumental artifacts by position matching. After the SAGE-Var source list was matched to the mosaic photometry, the original SAGE Epoch 1 and 2 archive data were matched individually as well, producing a final source list of 1 717 554 (LMC) and 457 760 (SMC) sources with up to 6 individual 3.6 and 4.5 μm observations, as well as mosaic photometry available in the longer wavelength IRAC bands. Table 2 lists the number of unique sources detected in each band of each epoch of SAGE-Var observations. Also listed is the number of objects detected in only one epoch, in two epochs, in three epochs, etc. A greater number of detections is preferable. The entire SAGE-Var data set, including all 6 epochs of observations in both bands, is available as an online table, hosted at the NASA/IPAC Infrared Science Archive[2].

---

[2] `http://irsa.ipac.caltech.edu/Missions/spitzer.html`

Table 2. Object Count

Epoch	LMC		SMC	
	3.6 μm	4.5 μm	3.6 μm	4.5 μm
Mosaic Photometry	1,712,135	1,712,994	454,951	455,587
SAGE Epoch 1	1,185,774	1,083,380	297,732	269,178
SAGE Epoch 2	1,163,888	1,068,438	290,055	262,408
SAGE-Var 1	1,177,715	824,928	289,359	185,392
SAGE-Var 2	1,242,129	852,734	264,921	176,911
SAGE-Var 3	1,244,543	855,533	287,168	173,756
SAGE-Var 4	1,244,791	845,370	280,656	172,379
1 Detection	116,285	240,980	56,602	78,408
2 Detections	197,701	240,983	75,528	61,853
3 Detections	270,324	273,872	79,241	65,429
4 Detections	253,951	183,972	54,222	45,670
5 Detections	271,603	180,249	64,538	43,291
6 Detections	593,727	391,448	120,822	73,748
Total Sources	1,717,554		457,760	

Note. — Summary of the number of unique objects detected in the SAGE-Var survey of the SMC and LMC

Table 3. Full Object Catalog Contents

Column	Name	Description	Null
1	desig	Source IRAC Designation	···
2	ra	Right Ascension, J2000 [deg]	···
3	dec	Declination, J2000 [deg]	···
4	e1_36	Epoch 1 flux in [3.6] band [Jy]	−99
5	e1_36_u	Uncertainty in Epoch 1 [3.6] flux [Jy]	−99
6–15	eN_36	Epoch 2–6 flux/uncertainty in [3.6] band[a] [Jy]	−99
16–27	eN_45	Epoch 1–6 flux/uncertainty in [4.5] band[b] [Jy]	−99
28	mean_36	Mean [3.6] flux [Jy]	−99
29	mean_36_u	RMS Uncertainty in mean [3.6] flux [Jy]	−99
30	mean_45	Mean [4.5] flux [Jy]	−99
31	mean_45_u	RMS Uncertainty in mean [4.5] flux [Jy]	−99
32–46	var_36_N	Variability index at [3.6] for interval[c] N	NaN
47–61	var_45_N	Variability index at [4.5] for interval[c] N	NaN
62	ogle_id	ID From the OGLE-III Catalog of Variable Stars	···
63	ogle_class	Classification from the OGLE-III CVS	···
64	ogle_per	Variability period from the OGLE-III CVS [days]	−99
65	macho_id	ID from the MACHO survey	···
66	macho_per	Variability period from the MACHO survey [days]	−99
67	grams_class	Classification of best fitting GRAMS model (C or O)	···
68	yso_class	'Y' if a source is classified as a YSO candidate	···

Note. — The full SAGE-Var catalog of 1 717 554 (457 760) sources in the LMC (SMC) is available from IRSA. This table is provided as a guide to the online catalog's structure and content.

[a] The epoch 2 through 6 [3.6] photometry follows the same format as columns 4 and 5

[b] The [4.5] photometry follows the same format as the [3.6] photometry in columns 4-15

[c] Defined in § 2.4 and Table 5

Table 4. Variable Object Catalog Contents

Column	Name	Description	Null
1	desig	Source IRAC Designation	···
2	ra	Right Ascension, J2000 [deg]	···
3	dec	Declination, J2000 [deg]	···
4	e1_36	Epoch 1 flux in [3.6] band [Jy]	−99
5	e1_36_u	Uncertainty in Epoch 1 [3.6] flux [Jy]	−99
6–15	eN_36	Epoch 2–6 flux/uncertainty in [3.6] band[a] [Jy]	−99
16–27	eN_45	Epoch 1–6 flux/uncertainty in [4.5] band[b] [Jy]	−99
28	mean_36	Mean [3.6] flux [Jy]	−99
29	mean_36_u	RMS Uncertainty in mean [3.6] flux [Jy]	−99
30	mean_45	Mean [4.5] flux [Jy]	−99
31	mean_45_u	RMS Uncertainty in mean [4.5] flux [Jy]	−99
32–46	var_36_N	Variability index at [3.6] for interval[c] N	NaN
47–61	var_45_N	Variability index at [4.5] for interval[c] N	NaN
62	ogle_id	ID From the OGLE-III Catalog of Variable Stars	···
63	ogle_class	Classification from the OGLE-III CVS	···
64	ogle_per	Variability period from the OGLE-III CVS [days]	−99
65	macho_id	ID from the MACHO survey	···
66	macho_per	Variability period from the MACHO survey [days]	−99
67	grams_class	Classification of best fitting GRAMS model (C or O)	···
68	yso_class	'Y' if a source is classified as a YSO candidate	···
69	amp_36	SAGE-Var observed [3.6] Amplitude	···
70	amp_45	SAGE-Var observed [4.5] Amplitude	···

Note. — This table extracts just those sources flagged as variable by the criteria of § 2.4. It follows essentially the same format as Table 3 with the addition of the observed amplitudes of the variable objects. These are simply the difference between the brightest and dimmest magnitudes observed for the source, and represent a lower limit on the source's full variability.

[a] The epoch 2 through 6 [3.6] photometry follows the same format as columns 4 and 5

[b] The [4.5] photometry follows the same format as the [3.6] photometry in columns 4-15

[c] Defined in § 2.4 and Table 5

2.4. Source Classification

Variables in the SAGE-Var dataset were identified using the variability criteria of Vijh et al. (2009). We calculate variability indices

$$V_{ij}^{b} = \frac{f_i^b - f_j^b}{\sqrt{(\sigma_i^b)^2 + (\sigma_j^b)^2}}$$

for every star, for every possible combination of epochs i and j, for the flux f in each SAGE-Var band b, ([3.6] and [4.5]) with photometric uncertainty σ. The photometric uncertainties are taken directly from the Wisconsin pipeline (§ 2.2). The variability index is thus the number of standard errors by which two epochs differ in brightness. Vijh et al. (2009) had only the first two epochs of the original SAGE survey, but 5 bands of photometry. In this study, our situation is reversed, in that we have only two bands of photometry, but $\binom{6}{2} = 15$ possible epochal differences. Each epochal difference probes variability on a different timescale (Table 5), and we term each epochal difference an *interval.* In order for a source to be classified as a variable in a given interval, we require it to exhibit 3σ flux variation in the same direction (that is, brightening or dimming) in both the [3.6] and [4.5] bands ($|V_{ij}^b| \geq 3$ and the same sign in both bands).

The SAGE-Var sample has a total of 819 sources in common with the sample of Vijh et al. (2009). Of these, we independently identify 752 (92%) as variables using our own criteria. The remaining 67 sources typically show marginally variable behavior, with variability indices very close to, but not quite exceeding, our 3σ level. We manually add to our catalog 66 of these 67 sources, omitting one source only detected in one of the four new epochs of SAGE-Var.

Table 5. Interval Timescales

Epochs	LMC Interval (days)	SMC Interval (days)	label
Epoch 1 − Epoch 2	100	96	1
Epoch 1 − Epoch 3	1854	793	2
Epoch 1 − Epoch 4	1878	819	3
Epoch 1 − Epoch 5	1984	922	4
Epoch 1 − Epoch 6	2107	1096	5
Epoch 2 − Epoch 3	1754	697	6
Epoch 2 − Epoch 4	1778	723	7
Epoch 2 − Epoch 5	1884	826	8
Epoch 2 − Epoch 6	2007	1000	9
Epoch 3 − Epoch 4	24	26	10
Epoch 3 − Epoch 5	130	129	11
Epoch 3 − Epoch 6	253	303	12
Epoch 4 − Epoch 5	106	103	13
Epoch 4 − Epoch 6	229	277	14
Epoch 5 − Epoch 6	123	174	15

Note. — By taking the difference between all possible combinations of observation epochs, we probe source variability on 15 timescales, from ∼1 month to ∼5.5 years. Throughout this paper, we refer to these epochal differences as intervals. The "label" column refers to the electronic table of the entire SAGE-Var catalog, available from the NASA/IPAC Infrared Science Archive (IRSA) (columns 32-61, Tables 3 & 4).

These criteria resulted in 2198 unique variables in the LMC along with 571 in the SMC. Histograms showing the number of sources seen as variable in each interval are shown in Figure 4. Intervals 1–9 show a generally higher number of detected variables because they all compare at least one of the initial two SAGE epochs to later observations. Taken during the cold *Spitzer* mission, which had a S/N approximately twice that obtained during the warm mission when all other epochs in SAGE-Var were taken. Interval 10 shows an unusually small number of variables because it is an order of magnitude shorter than any other interval, spanning only $\sim$20 days.

In order to classify the variables we did detect, we matched our detected variables against the OGLE-III Catalog of Variable Stars (CVS)[3], which consists of $\sim$150,000 classified variables in the LMC ($\sim$26,500 in the SMC) with well characterized variability information. Again using a $2''$ matching radius, we find 1361 OGLE-CVS matches to our 2198 SAGE-Var variables in the LMC, and 323 matches to our 571 variables in the SMC. These matches are shown in the $[3.6] - [4.5]$ vs. $[4.5]$ CMD in Figure 5. The OGLE populations we find in our data are detailed in Tables 6 & 7, along with the appropriate reference to the relevant OGLE-CVS document, if any.

LPVs, mainly evolved AGB stars, are the most numerous OGLE sources we detect in our sample. This is not surprising, as AGB stars are among the brightest objects in the IR sky, and many of our intervals probe timescales on which LPVs are expected to vary. We detect OGLE variables of every OGLE classification, down to nearly the limiting magnitude of our survey. These other classes tend to be blue in the diagrams of Figure 5, as the instability strip they occupy on the HR diagram places the peak of their SEDs blueward of the *Spitzer* bands.

---

[3] `http://ogledb.astrouw.edu.pl/~ogle/CVS/`

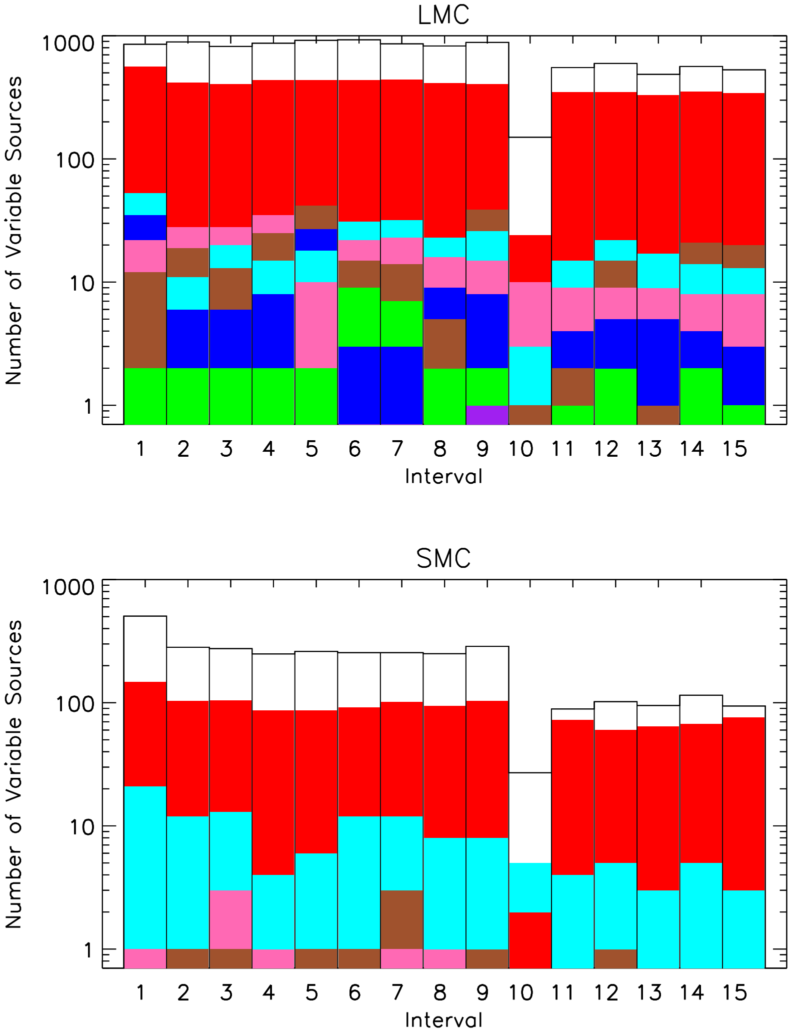

Fig. 4.— Histogram of the number of sources detected as variable in each interval of SAGE-Var. The top panel shows the source distribution in the LMC, while the bottom panel is that for the SMC. The colored portion of each bar represents the number of sources classified by the OGLE project. Red: LPVs, Cyan: Classical Cepheids, Hot Pink: Type II Cepheids, Blue: Eclipsing Binaries, Brown: YSOs, Green: R CrB stars, Purple: RR Lyrae stars. The white area at the top of each interval represents the unclassified variables seen in SAGE-Var but not listed in the OGLE-CVS (Figure 6). The labels for the intervals on the x-axis refer to the indices in Table 5. Classes are plotted from least numerous to most numerous, bottom to top.

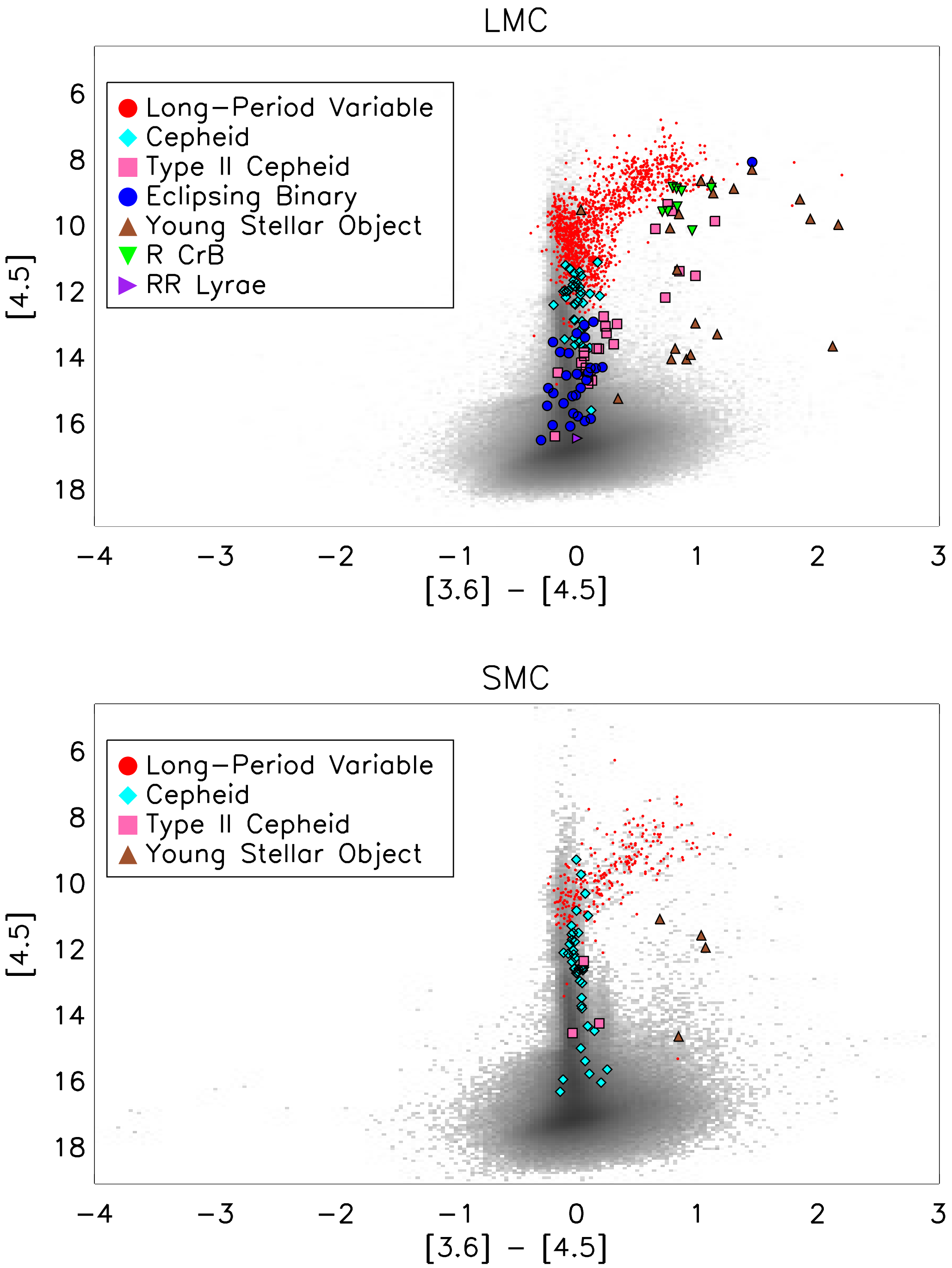

Fig. 5.— [3.6] – [4.5] vs. [4.5] CMD highlighting the OGLE-CVS variables with counterparts amongst the SAGE-Var classified variables. The LMC sources are shown in the top panel, and the SMC sources are shown in the bottom. The entire SAGE-Var catalog is shown as a gray-scale Hess diagram in the background. The same color scheme as in Figure 4 is used,

We also matched our data to the list of Young Stellar Object candidates (YSOs) in the LMC (SMC) compiled by Carlson et al. (2012) (Sewiło et al. 2013). We find 500 (337) YSOs in the entire SAGE-Var LMC (SMC) dataset, but only 12 (4) of them are identified as variables using our criteria. These are also shown in Figure 5.

Figure 6 shows the same CMDs as Figure 5 but highlighting the sources without counterparts in the OGLE CVS or MACHO survey. We remove any source with a SAGE [4.5] mosaic photometry dimmer than 15th magnitude identified as a variable but without an OGLE or MACHO counterpart. We include these sources in the online catalog for completeness, but data artifacts (such as blending with nearby sources) cause problems with our variability criteria in that regime. After removing those dim sources, we are left with 641(139) IR variables in the LMC (SMC) without OGLE or MACHO detected variation. There are a few extremely red sources in the AGB region of the CMD without OGLE identifications. Most of these sources are flagged as probable variables by the WISE survey, and our results bolster that conclusion (§ 3.1).

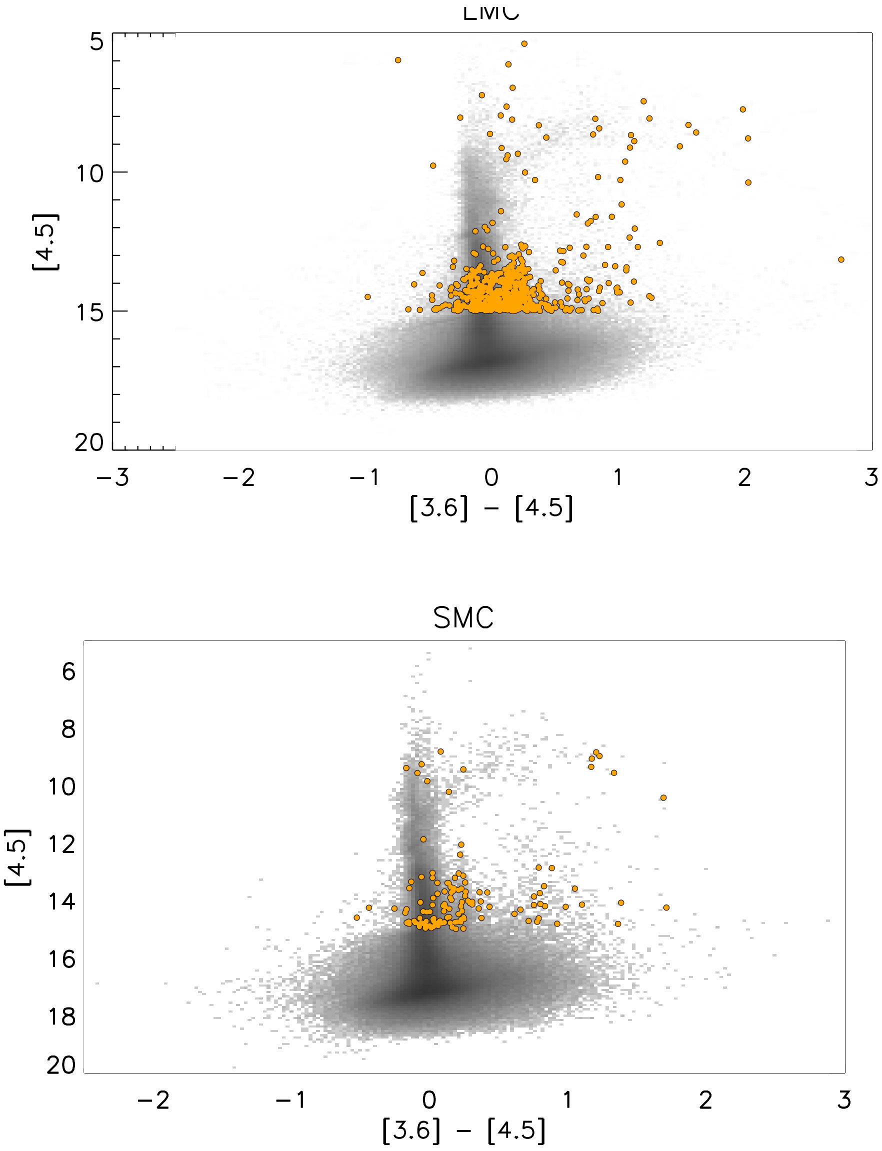

Fig. 6.— [3.6] − [4.5] vs. [4.5] CMD highlighting variables detected by SAGE-Var but not identified by the OGLE or MACHO surveys. The LMC sources are shown in the top panel, and the SMC sources are shown in the bottom. The entire SAGE-Var catalog is shown as a gray-scale Hess diagram in the background. To eliminate false positives due to low S/N, we only consider sources brighter than 15th magnitude to be variables.

Table 6. Variable populations detected in SAGE-Var LMC

Variable Classification	Number	Reference
Total Variables Detected	2198	
Long-Period Variables	1065	Soszyński et al. (2009b)
AGB C	5	
AGB O	6	
Mira AGB C	426	
Mira AGB O	143	
OSARG AGB C	15	
OSARG AGB O	42	
OSARG RGB C	1	
OSARG RGB O	17	
SRV AGB C	262	
SRV AGB O	148	
Cepheids	28	Soszyński et al. (2008a)
1O	1	
1O/2O	1	
F	26	
Type II Cepheids	19	Soszyński et al. (2008b)
BLHer	1	
RVTau	12	
WVir	6	
RR Lyrae	3	Soszyński et al. (2009a)
R CrB	6	Soszyński et al. (2009c)
Eclipsing Binaries	25	Graczyk et al. (2011)
EC	8	
ECL	1	
ED	8	
ESD	8	
Young Stellar Objects	12	Carlson et al. (2012)

Note. — This table lists the variable classifications and subclasses used by the OGLE Catalog of Variable Stars and the YSO catalog of

Carlson et al. (2012), and the numbers of such sources also detected as variable by the SAGE-Var survey in the LMC. A $2''$ matching radius was used for all OGLE catalog comparisons, and the YSO list was matched based on SAGE Archive designations. See the cited references for complete definitions of the subcategories listed here.

Table 7. Variable populations detected in SAGE-Var SMC

Variable Classification	Number	Reference
Total Variables Detected	571	
Long-Period Variables	276	Soszyński et al. (2011b)
Mira C	140	
Mira O	22	
OSARG C	7	
OSARG O	4	
SRV C	95	
SRV O	8	
Cepheids	42	Soszyński et al. (2010a)
F	40	
1O	2	
Type II Cepheids	3	Soszyński et al. (2010b)
RVTau	1	
WVir	1	
pWVir	1	
Young Stellar Objects	4	Sewiło et al. (2013)

Note. — This table lists the variable classifications and subclassifications used by the OGLE Catalog of Variable Stars and the YSO catalog of Sewiło et al. (2013), and the numbers of such sources also detected as variable by the SAGE-Var survey in the

SMC. A $2''$ matching radius was used for all OGLE catalog comparisons, and the YSO list was matched based on SAGE Archive designation.

3. RESULTS

3.1. New LPVs

Because they typically require large amounts of telescope time, most variability surveys are conducted in the optical, due to the expense of space-based multi-epoch observations. Ground-based variability surveys thus miss the reddest, most extreme LPVs, exactly the stars whose variability is most relevant to the evolved star dust budget because they dominate the mass return from LPVs to the ISM (Riebel et al. 2012; Boyer et al. 2012; Matsuura et al. 2009). SAGE-Var represents the first large scale variability survey at such red wavelengths. As such, we have the ability to detect as variable stars which have never been categorized as such before. Our survey detects 641 (139) sources in the LMC (SMC) which do not have well-defined variability measurements in the OGLE or MACHO surveys (Fig. 6). Some of these bright sources (10 in the LMC, 6 in the SMC) can be classified as AGB candidates, based on previous studies (Riebel et al. 2012), or their position in the $J - K_{\mathrm{s}}$ vs. K_{s} CMD. Figure 7 highlights these 10 (6) new LPV candidates against a Hess diagram of the entire SAGE-Var sample.

3.1.1. LMC AGB Candidates

We find 10 AGB candidates in the LMC without previously well-measured periods in either the OGLE or MACHO surveys. Most of these were flagged as highly likely to be true variables by the WISE survey, and we confirm that measurement. We do not find any of these 10 candidates in the SAGE-Spec (Kemper et al. 2010) list of LMC sources. We therefore employ an SED-based chemical classification. Using the GRAMS model grid (Sargent et al. 2011; Srinivasan et al. 2011), we classify 8/10 of them as C-rich AGB stars. C-rich AGB stars tend to be fainter in the optical than O-rich stars, and

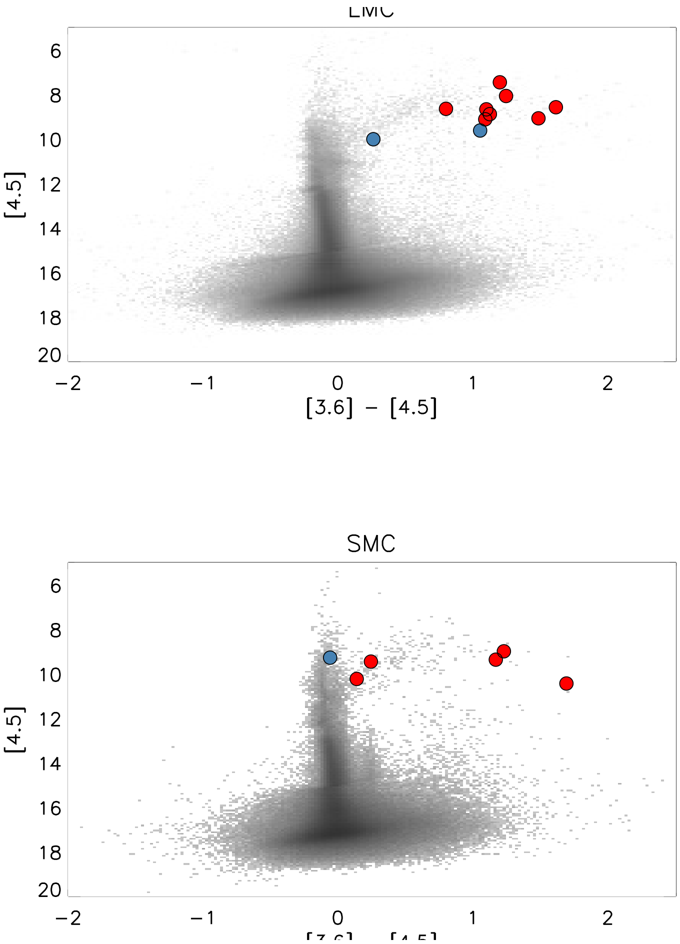

Fig. 7.— [3.6]−[4.5] vs. [4.5] CMD highlighting newly identified LPV candidates. The LMC sources are shown in the top panel, and the SMC sources are shown in the bottom. The entire SAGE-Var catalog is shown as a gray-scale Hess diagram in the background. Stars classified as C-rich by the GRAMS model grid are shown in red, stars classified as O-rich are shown in blue.

our newly measured variables skew red. AGB stars in our sample detected by the OGLE survey have an average $[3.6]-[4.5]$ color of -0.07 mag, while the sources with no OGLE detection are nearly a magnitude redder at these wavelengths, with an average $[3.6]-[4.5]$ of 0.74 mag. SAGE-Var has too sparse a sampling of the lightcurves to deduce a period for their variability, but we can place lower limits on their IR variability amplitudes. These sources are listed in Table 8.

3.1.2. SMC AGB Candidates

After cross-matching our list of AGB candidates in the SMC with SIMBAD and removing all sources confirmed to not be AGB stars, we generate a list of 6 new AGB candidates. We verified that none of these candidates were in the Ruffle et al. (2015, *in prep.*) list of spectroscopically classified SMC sources. Using the GRAMS model grid, we classify 5/6 of them as Carbon-rich. These sources are listed in Table 9. Source SSTISAGEMA J010041.61-723800.7 is the reddest new LPV candidate we idenitfy in the SMC. The best-fitting GRAMS model is an O-rich model, but the extreme redness of the source is more consistent with a C-rich star. Currently, the GRAMS model grid in the SMC places too much weight on the 24 μmphotometry, and this leads to some sources being mis-classified (see Srinivasan, et al. 2015, in prep for details). We manually change the classification of this source to C-rich.

3.2. Variability Amplitude and Dust Production Rate (DPR)

Le Bertre (1992) found a strong correlation between variability amplitude (measured in the K band), and $K-L'$ color for a sample of 20 carbon-rich LPVs in our galaxy. Whitelock et al. (1991) and Le Bertre (1993) found a similar correlation for O-rich LPVs.

Table 8. LPV Candidates in the LMC without OGLE or MACHO Variability Measurement

SAGE Designation[a]	RA (2000)	Dec (2000)	GRAMS Class	[3.6] Amplitude	[4.5] Amplitude	[3.6]–[4.5] color
J051041.21-683606.6	77.6717	-68.6018	C	0.83	0.85	1.24
J051414.85-700409.8	78.5619	-70.0694	C	0.93	0.86	1.12
J052503.26-692617.3	81.2636	-69.4381	C	0.90	0.69	1.48
J052813.02-691228.4	82.0543	-69.2079	C	0.86	0.75	1.09
J052900.19-695247.3	82.2508	-69.8798	C	1.11	0.52	0.80
J053051.75-694328.0	82.7156	-69.7245	C	1.42	1.19	1.20
J050202.38-690726.2	75.5099	-69.1239	C	0.52	0.56	1.10
J050718.89-683850.4	76.8287	-68.6474	C	1.50	1.27	1.61
J051913.89-693818.3	79.8079	-69.6384	O	0.29	0.31	0.26
J053010.30-690933.8	82.5429	-69.1594	O	0.36	0.30	1.05

[a] Designations in the online data table are prefaced with 'SSTISAGEMA'

Note. — The 10 AGB candidates in the LMC with variability newly detected by SAGE-Var. Many of these sources are confirmed to be AGB stars in the literature, but none have previously been observed to vary. The GRAMS Class column lists the classification (O-rich or C-rich) assigned each source by the GRAMS model grid (Riebel et al. 2012). The next two columns represent a lower bound on the IR variability amplitude of the sources, the maximum observed magnitude minus the minimum observed magnitude. The [3.6]–[4.5] color is also listed to connect the entries in this table to Figure 7.

Table 9. LPV Candidates in the SMC without OGLE or MACHO Variability Measurement

SAGE Designation[a]	RA (2000)	Dec (2000)	GRAMS Class	[3.6] Amplitude	[4.5] Amplitude	[3.6]–[4.5] color
J005106.28-731635.9	12.7762	-73.2767	C	0.34	0.34	0.14
J004544.12-720815.4	11.4338	-72.1376	C	0.32	0.40	0.24
J005926.35-722341.4	14.8598	-72.3949	C	1.09	0.88	1.23
J010232.75-721912.5	15.6365	-72.3202	C	1.08	1.06	1.17
J010041.61-723800.7	15.1734	-72.6335	C[b]	0.95	1.03	1.69
J005131.21-732007.7	12.8801	-73.3355	O	0.34	0.23	-0.06

[a] Designations in the online data table are prefaced with ‘SSTISAGEMA’

[b] The best-fitting GRAMS model for this source is an O-rich model with poor fit quality. Based on the extreme redness of this source, we classify it as C-rich

Note. — The 6 LPV candidates in the SMC with variability newly detected by SAGE-Var. Most of these sources are confirmed AGB stars, but none have previously been observed to vary. The GRAMS Class column lists the classification (O-rich or C-rich) assigned each source by the GRAMS model grid (Srinivasan, et al., 2015, in prep). The next two columns represent a lower bound on the IR variability amplitude of the sources, the maximum observed magnitude minus the minimum observed amplitude. The [3.6]–[4.5] color is also listed to connect the entries in this table to Figure 7.

Whitelock et al. (1994) found a strong correlation between the IR amplitude and the $K-[12]$ color. The K band is dominated by light from the stellar photosphere, while the [12] band represents the emission from the cooler dust shell around the star, and so this color serves as an indicator of the thickness of the circumstellar dust shell, and hence the rate of dust production by the star, if dust production rate is assumed to be constant.

By using the GRAMS modeling results of Riebel et al. (2012), we can directly compare the [3.6] amplitude and the DPR for our sample. Our results are shown in Figure 8. We extract every source in the SAGE-Var catalog with a valid GRAMS classification which was also classified as a true variable (§ 2.4). We see a slight correlation of increasing DPR with increasing infrared amplitude (albeit one with a very large scatter). C-rich and O-rich AGB stars have considerable overlap in their range of DPR, but more C-rich stars than O-rich stars extend to higher DPRs (Riebel et al. 2012). Because of this, the trend is more visible among the C-rich sources, but both populations follow the same basic trend, with considerably more scatter at low amplitudes for the O-rich sources.

3.3. PL Relationships

3.3.1. LPV PL Relationships

Combining the 6 epochs of the SAGE-Var survey allows us to calculate improved mean magnitudes for every source in the catalog. This is especially important for evolved variable stars such as those in the dataset of Riebel et al. (2010). The scatter in the period-luminosity relationships of those stars (Figures 1 & 2 in that paper) is ~0.3 mag, and is dominated by the intrinsic variability of the stars, not by the photometric extraction errors. Characterizing the AGB period-luminosity relationship is important in light of the upcoming launch of the James Webb Space Telescope (JWST). AGB stars are among the

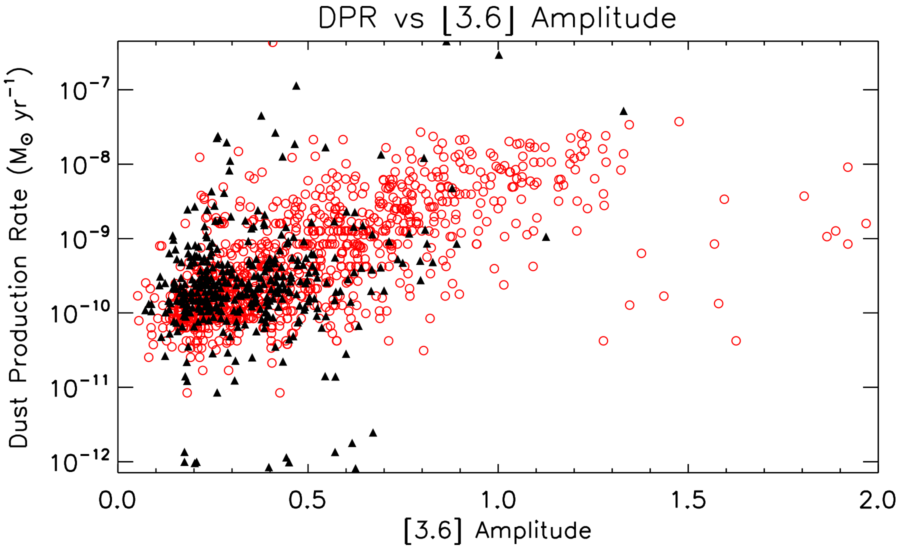

Fig. 8.— Dust Production Rate (DPR, $M_\odot$ yr^{-1}) vs [3.6] Amplitude for AGB stars in the LMC and SMC. The DPR is taken from the best-fitting GRAMS model, and the [3.6] Amplitude is defined as the dimmest measured SAGE-Var [3.6] magnitude minus the brightest [3.6] magnitude. C-rich AGB stars are shown as open red circles, and O-rich AGB stars as filled black triangles.

brightest sources in the IR sky, and with a large orbital platform concentrating on the IR, AGB stars could serve as important distance indicators, if their intrinsic luminosity can be well determined from their variability.

Figure 9 shows the period-magnitude relations constructed from the 6-epoch mean magnitudes constructed from the SAGE-Var data. We use AGB stars from the sample of Riebel et al. (2010) which are identified as variables in the SAGE-Var data to construct our relations. With observed variation, these stars benefit the most from the averaging process, compared to single random-phase observations. The 3.6 μm magnitude is used in the top panel, and the 4.5 μm band is used in the bottom. The periods come from the MACHO survey if possible, and from the OGLE survey if no MACHO period was available. The MACHO periods were given priority in order to maintain consistency with the study of Riebel et al. (2010). For those stars with measured periods in both the OGLE and MACHO surveys, the periods were found to differ by only 3 days on average. We only present updated fits for stars pulsating in the fundamental mode (sequence 1), as this was the only sequence with a significant population observed in SAGE-Var. The derived PL relations for the stars classified as O-rich (by the best-fitting GRAMS model) are shown in Figure 9 and quantitatively described in Table 10, which the fits to the stars identified as C-rich are shown in Figure 10 and described in Table 11.

Using the criteria described in Appendix A of Riebel et al. (2010), we identify three O-rich AGB stars in the SMC which lie on Sequence 1. We corrected for the difference in distance between the LMC and the SMC using distance moduli of 18.54 and 18.93, respectively (Keller & Wood 2006). These stars are plotted as pink crosses in Figure 9. On average, the LMC has a greater metallicity than that of the SMC. Our numbers are too small to from which to draw definite conclusions, but we do not see any evidence for a dependence of the LPV PL relation on metallicity in our sample. This idea is worthy of further investigation.

While we do see a slight decrease in the scatter about the best-fit line compared to that found by Riebel et al. (2010), the reduction is less than a factor of two, which leads us to believe much of this remaining scatter is intrinsic to the relationship and is not a product of observing different stars at different phases of their lightcurve.

We identified 223 (49) Carbon-rich, non-extreme AGB stars pulsating in the fundamental mode in the LMC (SMC). "Extreme" AGB stars are defined as those stars with $J--[3.6] > 3.1$. The J magnitude traces the emission from the stellar photosphere, while the [3.6] emission is from the circumstellar dust shell around these heavily enshrouded stars. At SAGE-Var wavelengths, these stars do not follow the same PL relation as less enshrouded stars because their brightness does not reflect stellar emission, but emission from the dust-shell (see figure 4 in Riebel et al. 2010). We eliminate these stars from this sample. The derived PL relations are shown in Figure 10 and quantitatively described in Table 11. The [4.5] data are shown for completeness, but we do not attribute any significance to the linear fits in that band. As discussed by Riebel et al. (2010), AGB stars are affected by a CO absorption feature in the [4.5] band which distorts the linear PL relationship in that band.

Correcting for distance, the SMC stars are well-mixed with the LMC stars, showing comparable scatter about the best-fit line. With many more samples than the O-rich, this provides more substantial evidence that C-rich AGB stars in the SMC follow the same PL relationship as those in the LMC.

Table 10. Period Magnitude Relationships for O-rich AGB stars Pulsating in the Fundamental Mode

PL Relation	N	scatter (mag)
This work:		
$[3.6] = -4.00(\pm 0.03) \log P + 20.24(\pm 0.07)$	131	0.18
$[4.5] = -3.78(\pm 0.03) \log P + 19.72(\pm 0.06)$	131	0.22
Riebel et al. (2010):		
$[3.6] = -3.41(\pm 0.04) \log P + 18.88(\pm 0.09)$	2221	0.271
$[4.5] = -3.35(\pm 0.04) \log P + 18.80(\pm 0.01)$	2227	0.270

Note. — PL relations for LPVs classified as O-rich AGB stars. The quoted scatter is the standard deviation of the residuals about the best-fit line.

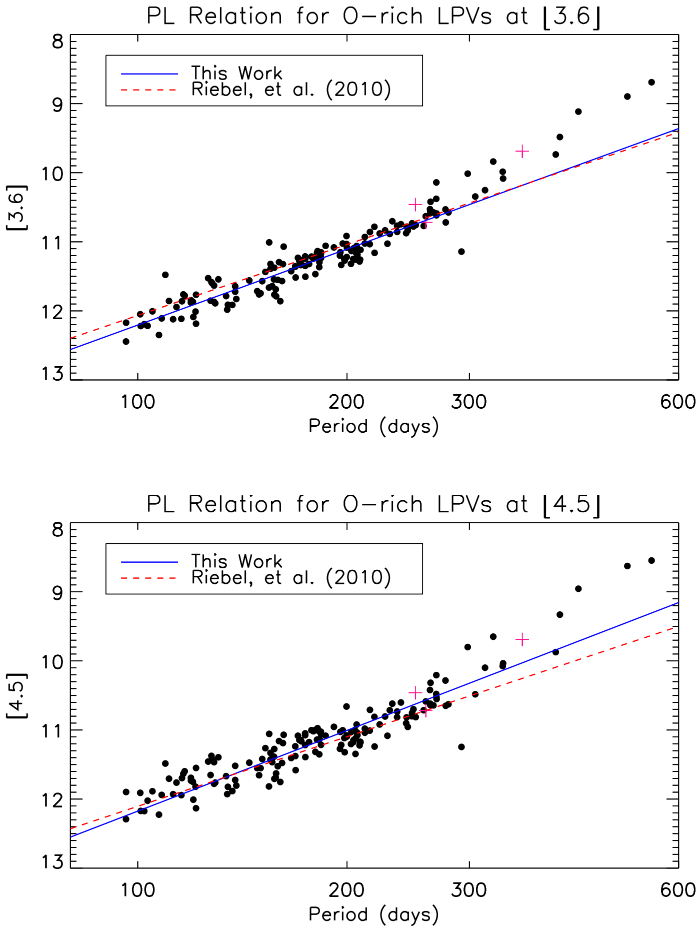

Fig. 9.— Period-Magnitude relationships for GRAMS classified O-rich AGB stars in the SAGE-Var sample, constructed using 6-epoch mean magnitudes in the [3.6] and [4.5] bands. Stars from the LMC are shown as black points, stars from the SMC shown as pink plus signs. Note the horizontal axis is a log scale.

Table 11. Period Magnitude Relationships for C-rich AGB stars Pulsating in the Fundamental Mode

PL Relation	N	scatter (mag)
This work:		
$[3.6] = -3.63(\pm 0.02) \log P + 19.11(\pm 0.05)$	272	0.24
$[4.5] = -3.84(\pm 0.02) \log P + 19.66(\pm 0.06)$	272	0.30
Riebel et al. (2010):		
$[3.6] = -3.77(\pm 0.05) \log P + 19.35(\pm 0.12)$	1813	0.251
$[4.5] = -3.56(\pm 0.05) \log P + 18.96(\pm 0.12)$	1816	0.265

Note. — PL relations for LPVs classified as C-rich AGB stars. The quoted scatter is the standard deviation of the residuals about the best-fit line.

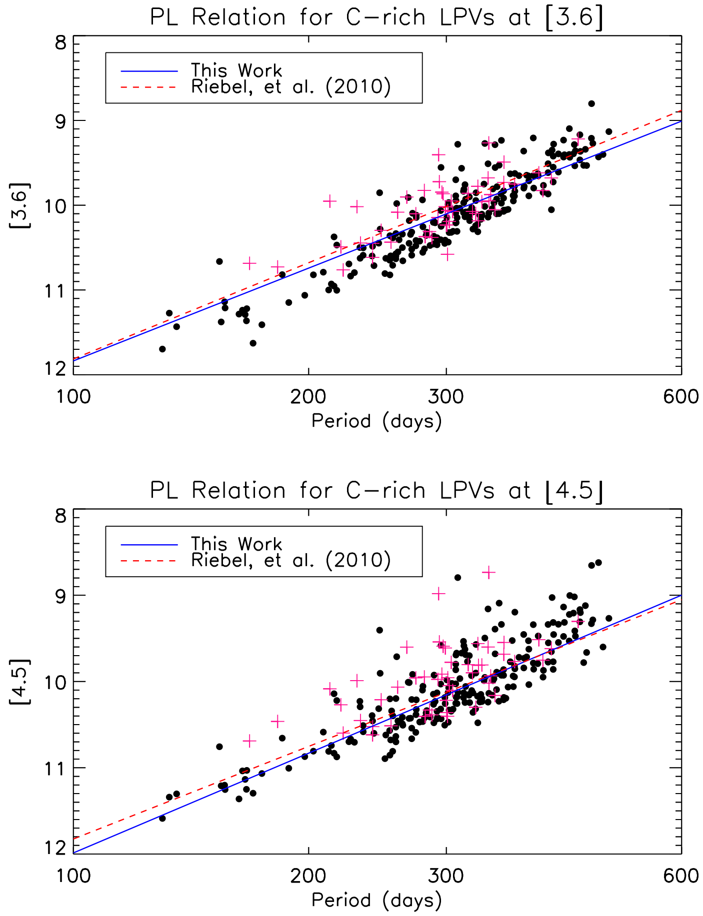

Fig. 10.— Period-Magnitude relationships for GRAMS classified C-rich AGB stars in the SAGE-Var sample, constructed using 6-epoch mean magnitudes in the [3.6] band. Stars from the LMC are shown as black points, stars from the SMC shown as pink plus signs. Note the horizontal axis is a log scale.

3.3.2. Cepheid IR PL Relationships

The well-known period-luminosity relationship of classical Cepheid variables is one of the most important extragalactic distance indicators in astronomy. Cepheid studies have generally focused on the optical, but McGonegal et al. (1982) pointed out that the near-IR offers several advantages for calibration of the Cepheid PL relation. Interstellar reddening, which imposes an intrinsic scatter on magnitude determinations in the optical, is much smaller at *Spitzer* wavelengths. Also, Cepheid variability amplitudes are considerably smaller in the IR, and thus sparsely sampled lighcurves are good tracers of the mean brightness. For these reasons, several recent surveys have focused on calibrating the Cepheid PL relation in the IR (Scowcroft et al. 2011; Freedman et al. 2012; Ngeow et al. 2012).

These studies have focused on small (∼80) samples of Cepheids, with well sampled light curves. SAGE-Var was designed as a more general variability survey, so what we lack in thorough coverage of the light-curve, we make up for in increased sample size. Based on OGLE classification, we find 837 (1536) fundamental mode Cepheids in our LMC (SMC) data.

We extract every source observed by SAGE-Var and classified as a fundamental mode Cepheid by the OGLE survey (Cepheids primarily varying in the first or higher overtone mode will, by definition, not lie on the primary PL relation). We eliminate any source with only one valid observation during SAGE-Var, as this provides limited means to constrain the uncertainty on the mean flux of the source. We calculate a simple mean magnitude for all our sources by averaging the fluxes of all SAGE-Var observations and then converting to magnitudes. Only 4 of our sources are in common with Scowcroft et al. (2011), and our mean magnitudes derived from randomly-phased observations are within 0.05 magnitudes of theirs.

The least squares linear fits (using 3σ clipping) are given below in Table 12. The

Leavitt Law at [3.6] derived from the LMC sample is illustrated in Figure 11 and the relation at [4.5] is shown in Figure 12. Fits are of the form $y = A \log P + B$, with y the mean magnitude of the source, and the period P measured in days. The scatter is defined as the standard deviation of the residuals to the fit. We visually inspected all the sources clipped as part of the fitting process. More than 90% are obvious blending/confusion issues in the original data. We find that when fitting the SMC data, using only sources with $\log P > 0.5$ provided a better visual fit to the data (following Scowcroft et al. 2011). The LMC fits were robust to this decision, and no period selection criteria were applied. The results given in Table 12 show the greater scatter about the SMC relationship compared with that in the LMC. This is due to the SMC's greater relative depth along the line of sight compared to the LMC (Caldwell & Coulson 1986). The slope of our [3.6] relations show very good agreement with those found by Freedman et al. (2012) in the LMC and by Ngeow et al. (2012) in the SMC. In the [4.5] band, we overplot the relations determined by Scowcroft et al. (2011), which also show good agreement with our own. As discussed by Scowcroft et al. (2011) and Monson et al. (2012), CO absorption in the [4.5] band renders this PL relation problematic for Cepheid distance determinations. This effect is clearly seen in Table 12, where the slopes of the PL relations at [3.6] in the the LMC and SMC agree well, while the slopes at [4.5] do not. This seems likely to be due to the different effects of CO absorption at different metallicities.

4. Conclusions

We present the results from a 4-epoch unbiased IR survey of the central regions of the LMC and SMC. We have produced full catalogs of our observations, consisting of 1 717 554 (457 760) objects in the LMC (SMC). We have identified 2198 (571) objects in the LMC (SMC) as probable variables.

Table 12. Classical Cepheid Period Luminosity relationships at [3.6] and [4.5] in the Magellanic Clouds

PL Relation	N	scatter (mag)
LMC:		
$[3.6] = -3.271(\pm 0.004)\log P + 15.993(\pm 0.003)$	811	0.13
$[4.5] = -3.157(\pm 0.004)\log P + 15.877(\pm 0.002)$	820	0.13
SMC:		
$[3.6] = -3.261(\pm 0.006)\log P + 16.511(\pm 0.004)$	452	0.18
$[4.5] = -3.437(\pm 0.004)\log P + 16.665(\pm 0.002)$	454	0.18

Note. — PL relations for fundamental mode classical Cepheids in the LMC and SMC. Fits were determined using a standard 3σ clipping procedure. The fits to the SMC data were determined by only considering Cepheids with $\log P > 0.5$. The scatter about the fit is defined to be the standard deviation of the residuals.

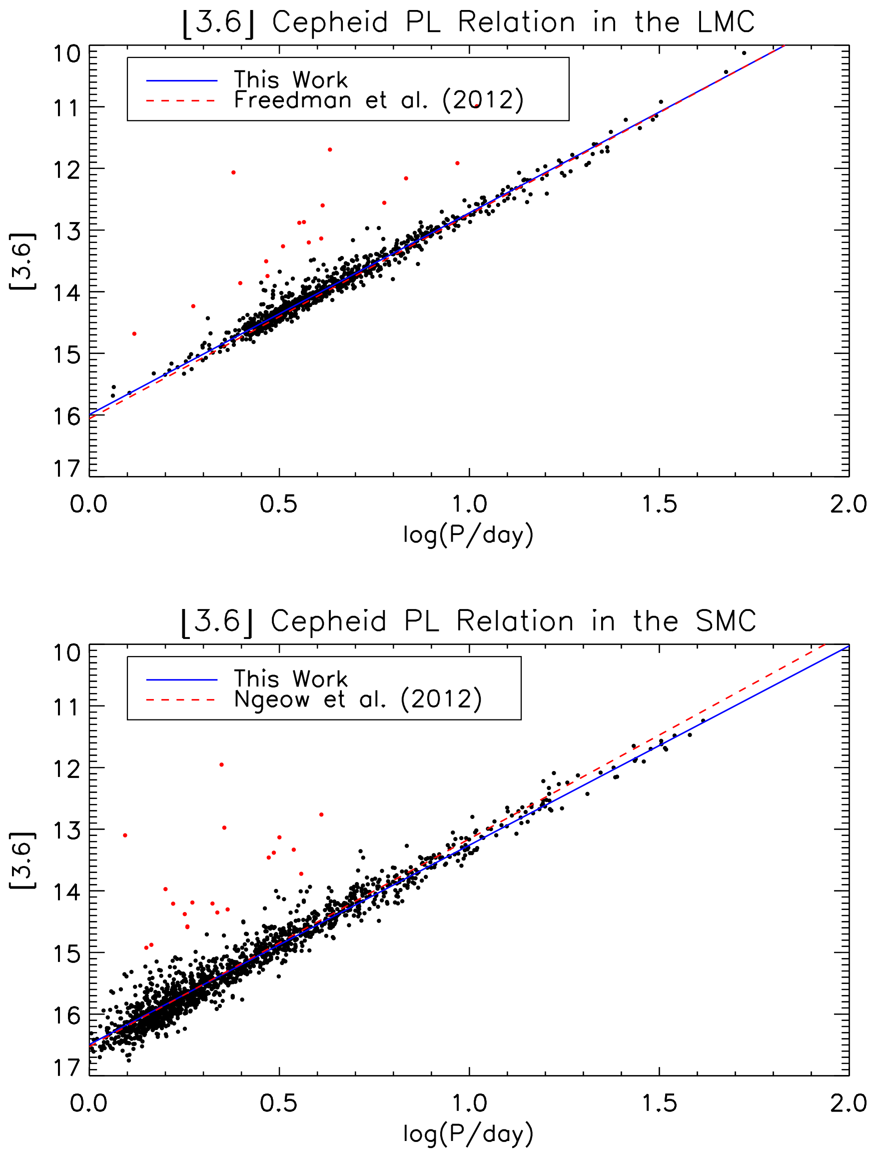

Fig. 11.— 3.6 μm Leavitt Law for 811 (452) classical Cepheids in the LMC (SMC). The LMC is shown in the top panel and the SMC in the bottom. The fits are quantitatively detailed in Table 12. Stars shown in red have residuals to the fit greater than 3σ and did not contribute to the fit. The relation derived in this study is plotted in blue. For the LMC (SMC) data, the relation determined by Freedman et al. (2012) (Ngeow et al. 2012) is overplotted in red as a dashed line.

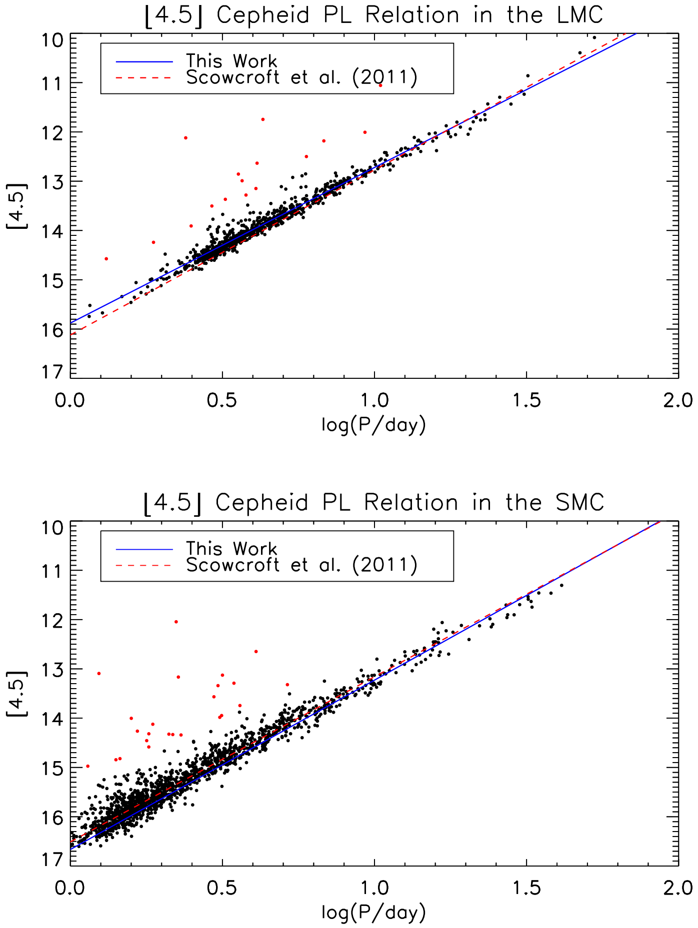

Fig. 12.— 4.5 μm Leavitt Law for 811 (452) classical Cepheids in the LMC (SMC). The LMC is shown in the top panel and the SMC in the bottom. The fits are quantitatively detailed in Table 12. Stars shown in red have residuals to the fit greater than 3σ and did not contribute to the fit. The relation derived in this study is plotted in blue. The relation determined by Scowcroft et al. (2011) using the original SAGE LMC data is overplotted in red as a dashed line.

We identify 10 (6) variable AGB candidates in the LMC (SMC) without well-determined variable periods from OGLE or MACHO (§ 3.1). Most of these sources were flagged as potential variables in the WISE survey, and our independent measurement confirms that probability.

Using mean magnitudes constructed from all available epochs of observations, we investigate the PL relationship for long-period variables oscillating in the fundamental mode. We find no significant reduction in the scatter about the best-fit relation compared to the results of Riebel et al. (2010), indicating the scatter (∼0.2 mag) might be intrinsic to the data (§ 3.3.1). We show that LPV stars in the SMC (Z∼0.04) and in the LMC (Z∼0.08) seem to follow the same PL relation.

We present infrared PL relations for a sample of 800 (400) Cepheids in the LMC (SMC). Cepheid amplitudes are small in the IR, and random-cadence results compare very well with those of Scowcroft et al. (2011), Freedman et al. (2012) and Ngeow et al. (2012) (§ 3.3.2).

5. Ackowledgements

This publication made use of the VizieR data base operated by CDS, Strasbourg, France. MWF and PAW gratefully acknowledge the receipt of research grants from the National Research Foundation (NRF) of South Africa.

Meixner acknowledges support from are grateful for support from NASA NAG5-12595, and Spitzer contract NM0710076.

This work is based on observations made with the *Spitzer* Space Telescope, which is operated by the Jet Propulsion Laboratory, California Institute of Technology under a contract with NASA.

MLB is supported by the NASA Postdoctoral Program at the Goddard Space Flight Center, administered by ORAU through a contract with NASA.

SS acknowledges support from the National Science Council and the Ministry of Science and Technology in the form of grant MOST103-2112-M-001-033-.

REFERENCES

Alcock, C., et al. 1997, ApJ, 486, 697

Benjamin, R. A., et al. 2003, PASP, 115, 953

Boyer, M. L., et al. 2015, ApJS, 216, 10

Boyer, M. L., et al. 2015, ApJ, 800, 51

Boyer, M. L., et al. 2012, ApJ, 748, 40

Boyer, M. L., et al. 2011, AJ, 142, 103

Caldwell, J. A. R., & Coulson, I. M. 1986, MNRAS, 218, 223

Carlson, L. R., Sewiło, M., Meixner, M., Romita, K. A., & Lawton, B. 2012, A&A, 542, A66

Freedman, W. L., Madore, B. F., Scowcroft, V., Burns, C., Monson, A., Persson, S. E., Seibert, M., & Rigby, J. 2012, ApJ, 758, 24

Glass, I. S., Ellis, R., Huchra, J., Kahn, S., Rieke, G., & Stetson, P. B. 1999, Handbook of Infrared Astronomy

Gordon, K. D., et al. 2011, AJ, 142, 102

Graczyk, D., et al. 2011, Acta Astron., 61, 103

Harris, J., & Zaritsky, D. 2004, AJ, 127, 1531

Hora, J. L., et al. 2004, Proc. SPIE, 5487, 77

Ita, Y., et al. 2002, MNRAS, 337, L31

Kemper, F., et al. 2010, PASP, 122, 683

Keller, S. C., & Wood, P. R. 2006, ApJ, 642, 834

Le Bertre, T. 1992, A&AS, 94, 377

Le Bertre, T. 1993, A&AS, 97, 729

Madore, B. F., & Freedman, W. L. 2005, ApJ, 630, 1054

Matsuura, M., et al. 2009, MNRAS, 396, 918

McGonegal, R., McAlary, C. W., Madore, B. F., & McLaren, R. A. 1982, ApJ, 257, L33

McQuinn, K. B. W., et al. 2007, ApJ, 664, 850

Meixner, M., et al. 2006, AJ, 132, 2268

Monson, A. J., Freedman, W. L., Madore, B. F., Persson, S. E., Scowcroft, V., Seibert, M., & Rigby, J. R. 2012, ApJ, 759, 146

Ngeow, C.-C., Citro, D. M., & Kanbur, S. M. 2012, MNRAS, 420, 585

Poleski, R., Soszyński, I., Udalski, A., Szymański, M. K., Kubiak, M., Pietrzyński, G., Wyrzykowski, Ł., & Ulaczyk, K. 2010, Acta Astron., 60, 179

Polsdofer, E., Seale, J., Sewiło, M., Vijh, U. P., Meixner, M., Marengo, M., & Terrazas, M. 2015, AJ, 149, 78

Riebel, D., Srinivasan, S., Sargent, B., & Meixner, M. 2012, ApJ, 753, 71

Riebel, D., Meixner, M., Fraser, O., Srinivasan, S., Cook, K., & Vijh, U. 2010, ApJ, 723, 1195

Sargent, B. A., Srinivasan, S., & Meixner, M. 2011, ApJ, 728, 93

Schlegel, D. J., Finkbeiner, D. P., & Davis, M. 1998, ApJ, 500, 525

Scowcroft, V., Freedman, W. L., Madore, B. F., Monson, A. J., Persson, S. E., Seibert, M., Rigby, J. R., & Sturch, L. 2011, ApJ, 743, 76

Sewiło, M., et al. 2013, ApJ, 778, 15

Soszyński, I., et al. 2008a, Acta Astron., 58, 163

Soszyński, I., et al. 2008b, Acta Astron., 58, 293

Soszyński, I., et al. 2009a, Acta Astron., 59, 1

Soszyński, I., et al. 2009b, Acta Astron., 59, 239

Soszyński, I., et al. 2009c, Acta Astron., 59, 335

Soszyński, I., et al. 2010a, Acta Astron., 60, 17

Soszyński, I., Udalski, A., Szymański, M. K., Kubiak, M., Pietrzyński, G., Wyrzykowski, Ł., Ulaczyk, K., & Poleski, R. 2010b, Acta Astron., 60, 91

Soszyński, I., Udalski, A., Szymañski, M. K., Kubiak, J., Pietrzyński, G., Wyrzykowski, Ł., Ulaczyk, K., & Poleski, R. 2010c, Acta Astron., 60, 165

Soszyński, I., et al. 2011b, Acta Astron., 61, 217

Srinivasan, S., Sargent, B. A., & Meixner, M. 2011, A&A, 532, A54

Udalski, A., Kubiak, M., & Szymanski, M. 1997, Acta Astron., 47, 319

Vassiliadis, E., & Wood, P. R. 1993, ApJ, 413, 641

Vijh, U. P., et al. 2009, AJ, 137, 3139

Whitelock, P., Feast, M., & Catchpole, R. 1991, MNRAS, 248, 276

Whitelock, P., Menzies, J., Feast, M., Marang, F., Carter, B., Roberts, G., Catchpole, R., & Chapman, J. 1994, MNRAS, 267, 711

Whitelock, P. A., Feast, M. W., van Loon, J. T., & Zijlstra, A. A. 2003, MNRAS, 342, 86

This manuscript was prepared with the AAS LaTeX macros v5.2.